2020

Characterization of Coal Particles in the Soil of a Former Rail Yard and Urban Brownfield: Liberty State Park, Jersey City (NJ), USA

Diane F. Hagmann
Montclair State University

Michael A. Kruge
krugem@mail.montclair.edu

Nina M. Goodey
Montclair State University

Jennifer Adams Krumins
Montclair State University

Hagmann D.F., Kruge M.A., Goodey N.M., Krumins J.A. (2020) Characterization of coal particles in the soil of a former rail yard and urban brownfield: Liberty State Park, Jersey City (NJ), USA. International Journal of Coal Geology 217:103328. https://doi.org/10.1016/j.coal.2019.103328. (http://www.sciencedirect.com/science/article/pii/S0166516219307001)

Characterization of coal particles in the soil of a former rail yard and urban brownfield: Liberty State Park, Jersey City (NJ), USA

Diane F. Hagmann[1], Michael A. Kruge[1]*, Nina M. Goodey[2,3], Jennifer Adams Krumins[4]

[1]Dept. of Earth & Environmental Studies, Montclair State University, Montclair, NJ 07043 USA

[2]Dept. of Chemistry & Biochemistry, Montclair State University, Montclair, NJ 07043 USA

[3]PSEG Institute of Sustainability Studies, Montclair State University, Montclair, NJ 07043 USA

[4]Dept. of Biology, Montclair State University, Montclair, NJ, USA

*Corresponding author. krugem@montclair.edu

Abstract

From the 1850's until the 1960's, the Central Railroad of New Jersey was among several major railways shipping anthracite and bituminous coal to the New York City area, transferring coal from railcar to barge at its extensive rail yard and port facility in Jersey City. The 490 ha Liberty State Park was developed on the site after the rail yard closed, but a ca. 100 ha brownfield zone within the park remains off limits to visitors pending future remediation. As part of an environmental forensic and industrial archeological investigation of this zone, the present study characterizes anthracite and bituminous coal particles present in abundance in the soil by scanning electron microscopy (SEM) and pyrolysis-gas chromatography-mass spectrometry (Py-GC-MS). A simple pretreatment procedure employing density separation improved the analytical results. This detailed information about the nature of contaminants at the site will help to inform the remediation effort in the public interest.

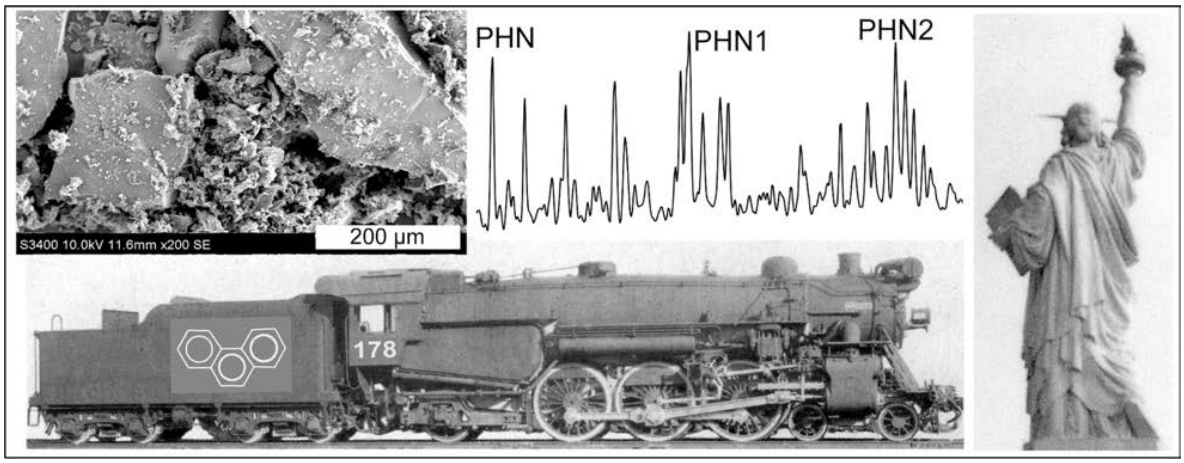

Graphical abstract

Keywords

environmental forensics, coal, Liberty State Park, brownfield remediation, pyrolysis-gas chromatography-mass spectrometry (Py-GC-MS), density separation

Highlights

- Legacy coal contamination is widespread in the soils of an unremediated restricted area within Liberty State Park (New Jersey, USA), formerly a major rail yard and port for coal shipment.
- The coal particles in the soil are mostly of anthracite rank, the low PAH content of which reduces the potential environmental hazard at this brownfield site.
- PAH-rich bituminous coal particles, while less abundant, may be of greater environmental concern, although the degree of bioavailability of their constituent PAHs must be considered.
- Analysis of soil components by pyrolysis-gas chromatography-mass spectrometry (Py-GC-MS) after a preparative density separation procedure is shown to an effective environmental forensics tool.

Declarations of interest: None

1. Introduction

The Central Railroad of New Jersey (CRRNJ) was one of several major private railways operating from the mid-19th to the mid-20th century with an eastern terminus on New York Harbor and the Hudson River in the U.S. state of New Jersey (Figs. 1, 2). Typical of these

intermodal operations, the CRRNJ transported freight and passengers from the interior to a vast rail yard along the shore for transfer to barges and ferries, respectively, for connection across the water to nearby New York City and points east (Anderson, 1984). Due to unfavorable economic conditions, including competition from highway transportation, all of these private railways ceased operations during the mid-20th century. Some of the lines were subsequently incorporated into the New Jersey Transit regional system, which still maintains a rail-to-ferry passenger service out of the historic station in Hoboken (NJ). CRRNJ's Jersey City station was restored as a tourist attraction but no longer operates, as the tracks were removed when the rail yard was abandoned in the late 1960's and subsequently converted into Liberty State Park (LSP) (Gallagher et al., 2008a; b). The park takes its name from the iconic Statue of Liberty, situated about 600 m across the water at its closest point, allowing park visitors a dramatic view of the rear of the colossus.

Figure 1

Figure 2

Coal transport was a major component of CRRNJ operations, for example, producing about 26 % of the company's total revenue in 1943, with 28 % of the coal moving via Pier 18 and its dedicated network of tracks at that time (Figs. 2, 3). The railroad conveyed anthracite coal (Fig. 3A) from its own mines in eastern Pennsylvania and also hauled bituminous coal trains originating further west belonging to other companies. Relative tonnages of anthracite and bituminous coals were roughly the same, varying over time with market demand. Arriving at Pier 18, massive coal dumping structures transferred the cargo to waiting coal barges (Figs. 3B-D) (Anderson, 1984).

Figure 3

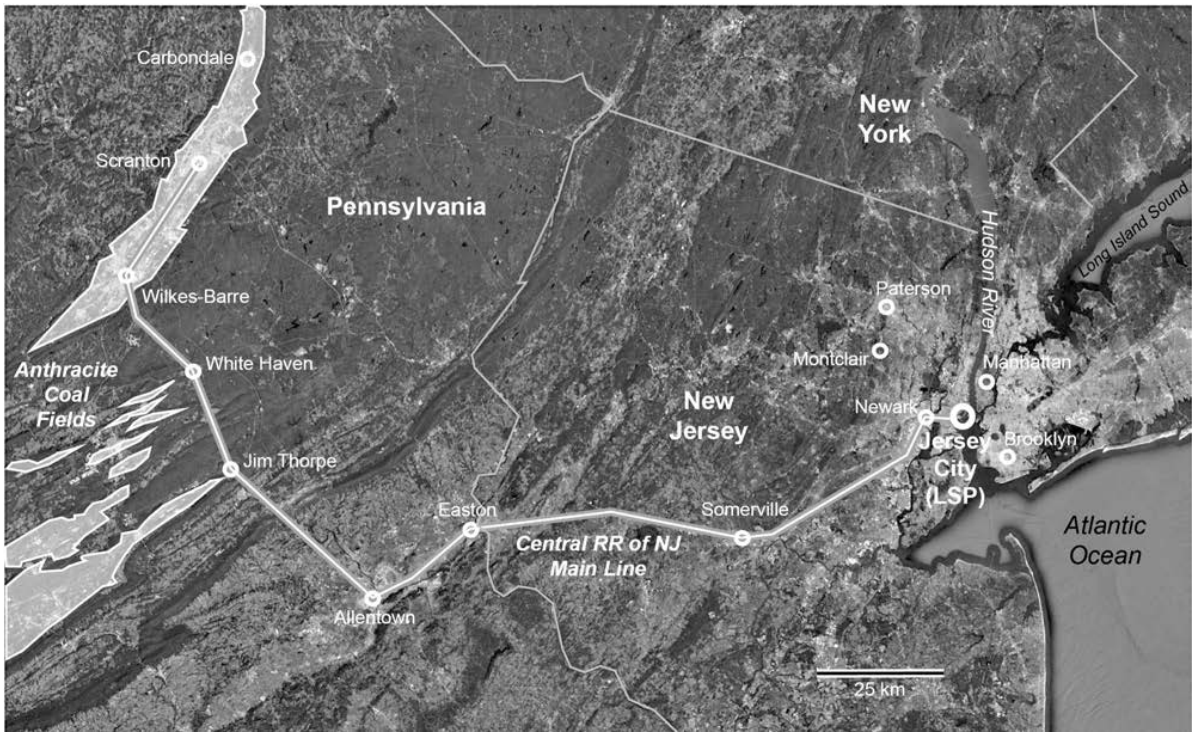

Figure 1. Index map showing location of Liberty State Park (LSP) in Jersey City (NJ), USA, the principal anthracite coal fields of Pennsylvania, and the former Central Railroad of New Jersey main line. Base map: Google Earth; coalfields: Pennsylvania Dept. of Environmental Protection; rail line: Anderson (1984).

(2 Column)

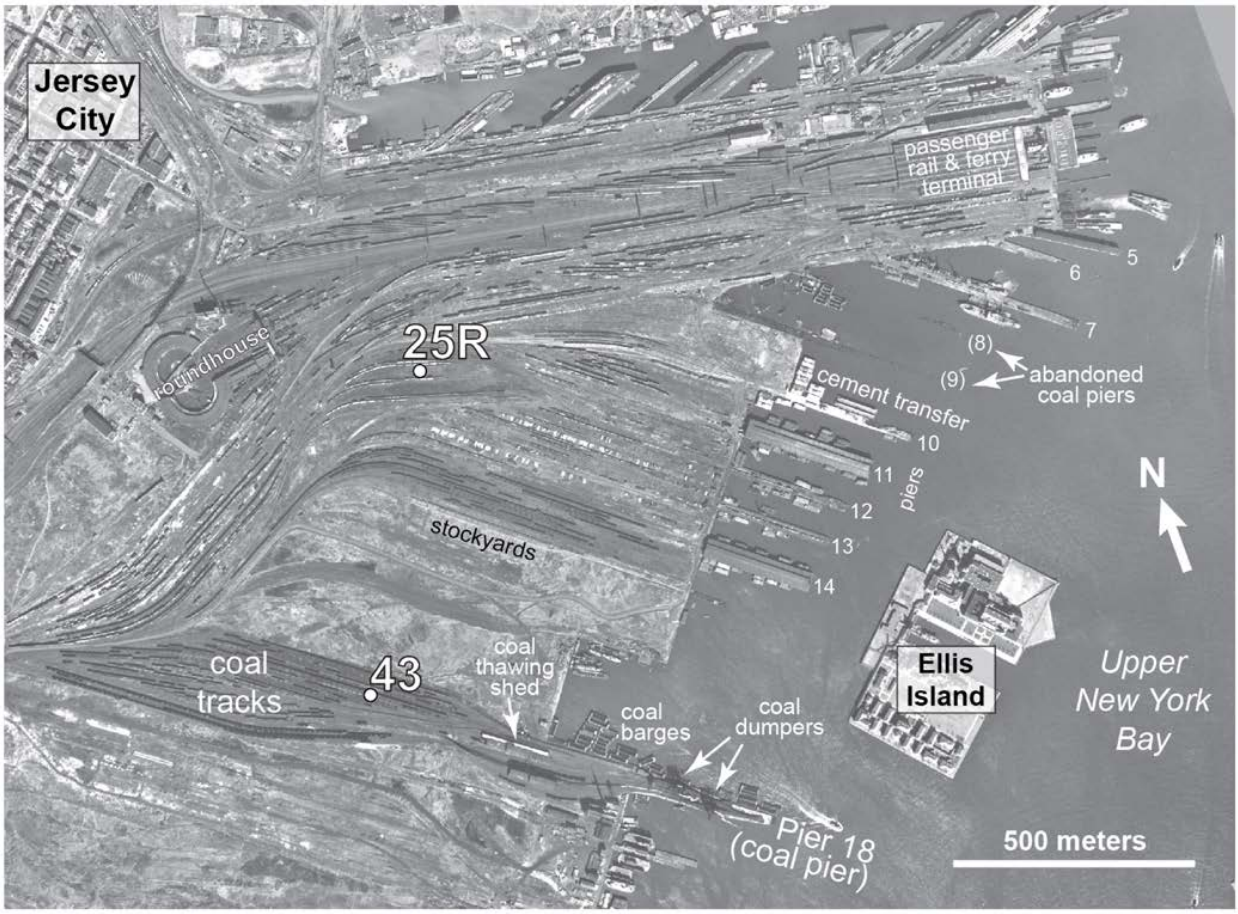

Figure 2. The Central Railroad of New Jersey's rail yard and marine terminal in Jersey City as it appeared in a 1954 aerial image, overprinted with the location of the two soil samples (25R, 43) presented in this study. At the time of the photograph, coal transport operations were largely confined to the zone seen in the lower part of the image, on the tracks leading to Pier 18. Note the locations of the passenger terminal and roundhouse. Base image: U.S. Geological Survey; identification of coal handling facilities: Anderson (1984); pier identification: Brooklyn Historical Society Archives.

(2 Column)

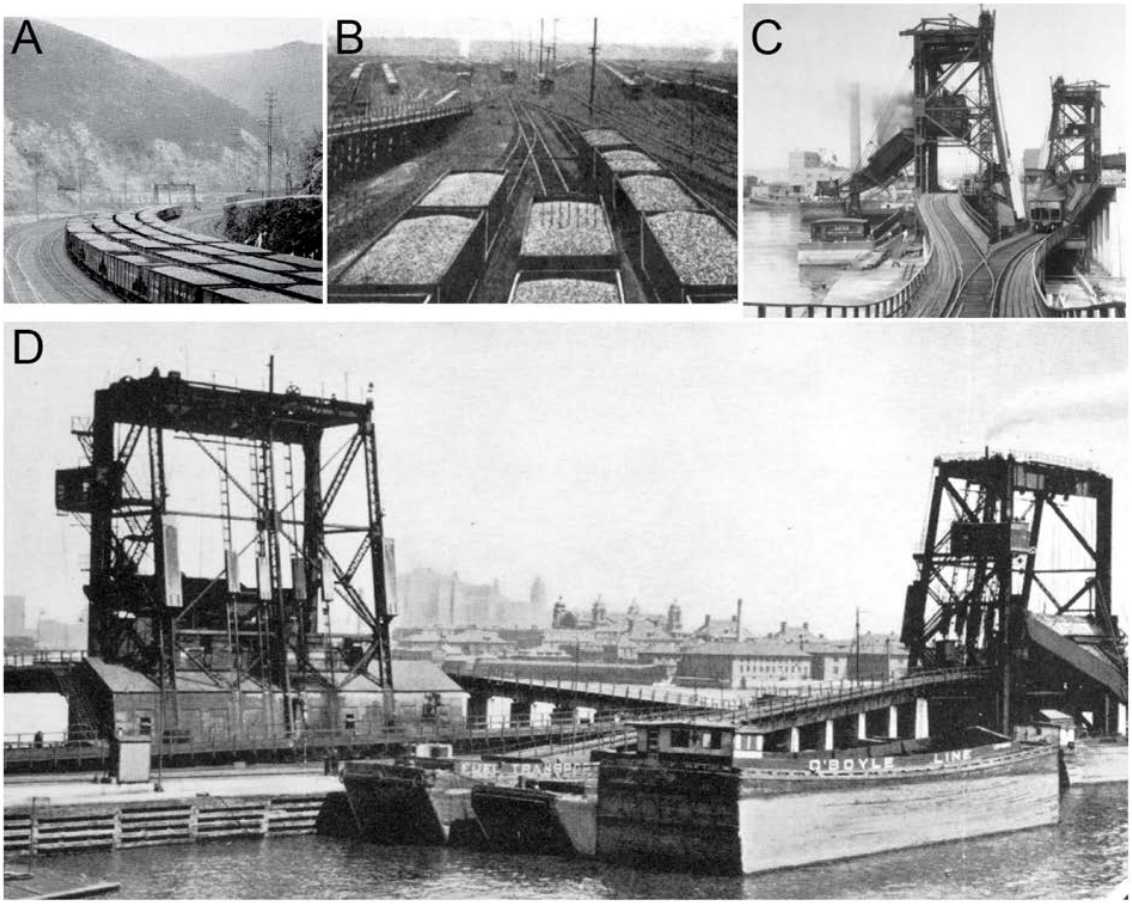

Figure 3. Historical images of CRRNJ coal transport operations in the 1940's. (A) Loaded coal trains in Jim Thorpe, Pennsylvania (Fig. 1; town formerly known as Mauch Chunk). (B) Loaded coal cars approach Pier 18 in the Jersey City rail yard. View to the west showing the yard's track network (Fig. 2). (C) View of Pier 18's two coal dumping towers for transfer of coal from railcar to barge. View is to the west from the eastern end of the pier. (D) View to the northeast of Pier 18's coal dumpers. Note Ellis Island in the background. Photos: Anderson (1984); used with permission.

(2 Column)

After the rail yard and its piers were closed and dismantled, the state of New Jersey acquired the land and created the 490 ha Liberty State Park. About 100 ha of the park remains an unremediated brownfield site, off limits to the public and constituting the study area of this project (Fig. 4A). In recent years, the site's botanical succession, soil microbiology, and contaminant geochemistry have been extensively studied (e.g., Gallagher et al., 2008a; b; 2018; Hagmann et al., 2015; 2019; Krumins et al., 2015; Singh et al., 2019a; b). In spite of evident inorganic and organic contamination, including abundant visible coal fragments in the soil, most of the restricted zone supports lush plant life, the product of natural, passive revegetation over a half century (Figs. 4B, C).

Figure 4

Unburned coal, particularly of high volatile bituminous rank, contains high concentrations of polycyclic aromatic hydrocarbons (PAHs) among other compounds (Stout and Emsbo-Mattingly, 2008; Laumann et al., 2011). While PAHs in soils may affect plant health (Brooks, 2004; Smith et al., 2006), the extent to which this is an environmental concern in this case is linked to the degree of PAH bioavailability and biodegradability if sequestered within coal particles in soil (Stout and Emsbo-Mattingly, 2008; Yang et al., 2008a; b; Achten and Hofmann, 2009; Achten et al., 2011; Fabiańska et al., 2016; Hindersmann and Achten, 2018; Nádudvari et al., 2018a; b). Hagmann et al. (2019) undertook an environmental forensic investigation of coal-contaminated soils from the LSP brownfield site, describing in detail the distribution of saturated and aromatic hydrocarbons, heavy metals, and coal macerals. However, they used only the < 2 mm particle size fraction, to the exclusion of the visible coal particles evident during field sampling. The present study re-examines soils from two of the investigated

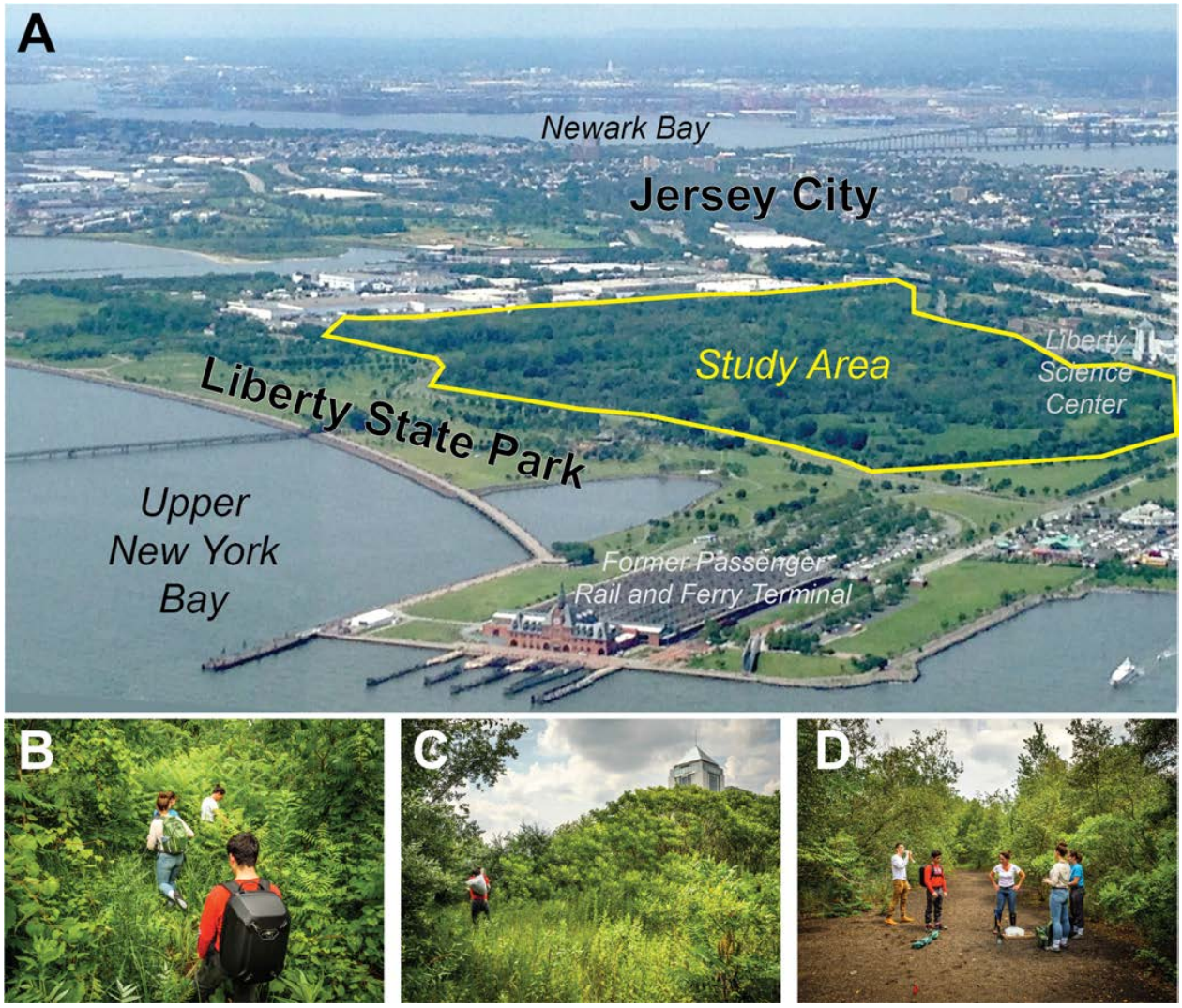

Figure 4. Appearance of Liberty State Park in 2017. (A) Aerial view towards the southwest showing the study area within the park. Note the former passenger rail and ferry terminal, partially restored but non-functioning, and the Liberty Science Center museum, built on the site of the former railroad roundhouse (Fig. 2). Photo: D. Hagmann. (B, C) Dense vegetation covers most of the study area. The top of the Liberty Science Center tower appears in C. (D) Soil sample 25R was collected from this anomalously barren strip within the study area. Photos B-D: M. Peters, Montclair State Univ.; used with permission.

(2 Column. Grayscale in print edition; color in online edition.)

sampling locales within LSP (Fig. 2), this time considering the full particle size range with emphasis on coal, to aid in future remediation of the brownfield.

Micro-scale analytical pyrolysis-gas chromatography-mass spectrometry (Py-GC-MS) has been shown to provide a rapid, reproducible means of chemically characterizing a wide variety of solid organic matter types with minimal sample preparation (Wampler, 2007). Py-GC-MS has increasingly been applied to environmental investigation of soils and sediments (summarized in Kruge, 2015), specifically including brownfield studies (Lara-Gonzalo et al., 2015) and environmental forensics (Kruge et al., 2018). It is utilized here for the direct, qualitative characterization of coal particles and coal-contaminated soil.

Sedimentary petrologists have long favored density separation for isolating heavy minerals from sandstones for microscopic evaluation (e.g., Boggs, 2009). It has also been employed extensively in coal studies, evolving into the use of the sophisticated analytical technique of density gradient centrifugation for the separation of coal and kerogen macerals (e.g., Dyrkacz and Horwitz, 1982; Crelling, 1988; 1989; Stankiewicz et al., 1994a;b; Kruge et al., 1997). In the present study, a simple floatation method was employed to isolate soil organic matter and various coal types to improve the chemical characterization results.

The restricted zone of LSP is slated for gradual remediation into managed wetland, grassland, and forest with public access (McDonald, 2018). The environmental forensic and industrial archeological approach of the present study will help to inform the remediation effort in the public interest.

2. Methods

2.1. Site description

Soils for this study were collected within LSP in Jersey City (NJ, USA) include soil from vegetated Site 43, formerly beneath a railroad track, and soil from Site 25R taken on what remains an anomalously barren strip of land formerly between railroad tracks (Figs. 1-4). These sites are inside the unremediated, restricted-access 100-ha zone of the park. The railroad tracks and their crossties were removed around the time the railyard was abandoned in the late 1960s. Since the railyard was abandoned, a dense forest consisting mostly of hardwood and herbaceous assemblages naturally grew within the restricted-access area (Gallagher et al., 2008a; b) (Figs. 4A-C).

2.2. Soil collection

Soil was collected from LSP sites 43 and 25R from below the leaf litter to a depth of 10 cm and stored in at 4 °C. Sample coordinates were determined by reference to Global Positioning System (GPS) satellite signals in the field, transferred to aerial imagery using the Google Earth application, and carefully matched by graphical overlay to the 1954 aerial image (Fig. 2) in the U.S. Geological Survey archives (earthexplorer.usgs.gov) as previously detailed (Hagmann et al., 2019).

2.3. Hand-picked coal and plant material

Vegetation detritus from LSP site 43 was hand-picked from whole soil. This plant material, which consisted of roots and twigs, were rinsed in deionized (DI) water and dried (40 °C overnight). In another procedure, soil samples from sites 25R and 43 were wet-sieved through a 2 mm sieve and sonicated in DI water. The > 2 mm fraction was further separated into the following categories based on visual inspection under a binocular microscope: coal, coke,

and combustion spherules. Coal particles from both sites (2 to 10 mm in size) were designated for further processing, as described in Sections 2.4 and 2.6 (Fig. 5).

Figure 5.

2.4. Scanning electron microscopy (SEM)

Before SEM, the hand-picked coal particles were individually air-dried and gently crushed using a mortar and pestle. Fragments of a single coal particle were spread on the carbon tape and then loaded on the SEM sample stub. After applying a thin layer of carbon film under a Denton Desk 4 coater, the fragments were observed by the Hitachi S-3400N SEM and with Bruker –AXS Energy Dispersive X-Ray Spectroscopy (EDS) detector.

2.5. Soil separation by density

Soils from both sites were also separated based on density (Fig. 5). First, dried whole soil (40 °C overnight) was ground using a mortar and pestle to pass through a 1 mm sieve. A 5 g aliquot was placed in 10 mL of DI water (1.0 g/mL) and the floating material after centrifugation was collected (Fraction 1). An aqueous potassium iodide (ACS Reagent Grade, Ricca Chemical, Fisher Scientific) solution (1.6 g/mL in DI water, 10 mL) was added to the remaining soil (i.e., the sink material after Fraction 1 was removed). The particles that were floating after centrifugation were collected in filter paper and rinsed with DI water (Fraction 2). Finally, the remaining residue was rinsed with DI water and collected (Fraction 3). For each fraction, the suspension was thoroughly mixed and then centrifuged at 4,000 rpm for 15 minutes. Aliquots of Fraction 3 residues were analyzed by SEM, following the procedure outlined in Section 2.4. Fraction 1 was predicted to contain the natural biomass that floats in water, Fraction 2 was

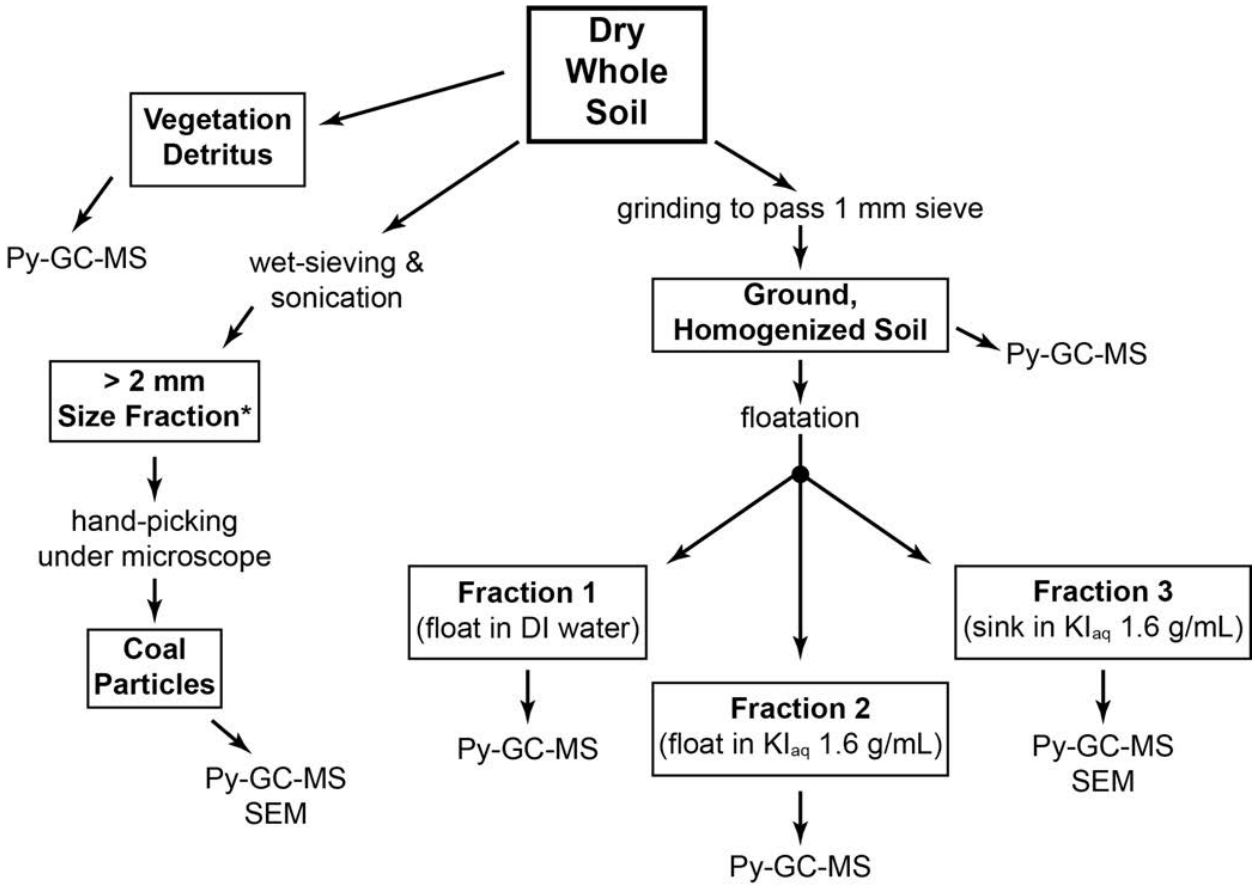

Figure 5. Experimental flow chart. See section 2 for details. No vegetation detritus was picked from barren site 25R soil. * < 2 mm size fraction previously studied in detail (Hagmann et al., 2019).

(One column)

expected to include the coal particles that float in the dense aqueous KI solution, while Fraction 3 should include the soil mineral matter that is too dense to float in either liquid.

2.6. Pyrolysis-Gas Chromatography-Mass Spectrometry (Py-GC-MS)

The hand-selected vegetation detritus was crushed using a mortar and pestle and analyzed by Py-GC-MS (Fig. 5). Several of the hand-picked coal particles were individually crushed using a mortar and pestle and separately analyzed by Py-GC-MS. These included ten individual coal particles from site 43 and three coal particles from site 25R. Whole soil samples and each of the three fractions separated by density from LSP sites 43 and 25R were also pyrolyzed. For quality control, Py-GC-MS of the 25R whole soil was performed twice. Py-GC-MS was accomplished using a CDS 5150 Pyroprobe (CDS Analytical Inc., Oxford, PA) coupled to a Thermo Finnigan Focus DSQ GC/MS (Thermo Electron Corporation, Madison, WI) equipped with an Agilent DB-1MS column (30 m × 0.25 mm i.d. × 0.25 μm film thickness). The GC oven temperature was programmed from 50 °C to 300 °C (at 5 °C min^{-1}), with an initial hold of 5 min at 50 °C and a final hold of 15 min at 300 °C. Pyrolysis was performed for 20 s at 610 °C. The MS was operated in full scan mode (50-500 Da, 1.08 scans s^{-1}). The MS was calibrated by autotuning with PFTBA and blanks were run each day before samples were analyzed. Compounds were identified using the W8N08 mass spectral library (John Wiley and Sons, Inc., New York, NY), the online NIST Standard Reference Database Number 69 (webbook.nist.gov/chemistry/), and by reference to the literature. For this study, no internal or external standards were employed, thus no attempts at quantitative determination were made.

3. Results and discussion

3.1. SEM of coal particles

Hand-selected coal particles from the > 2 mm fraction of soil from LSP site 43 were imaged using SEM, revealing surface encrustations that had resisted sonication (Fig. 6). The EDS mapping indicated that the encrustations like those imaged in Figure 7 are aluminosilicate phases (strong Si, Al, and O spectral signals) adhering to the coal. The overlapping spectral signals (Fig. 7B) can more clearly be seen in the individual mapping of Al and Si (Figs. 7C, D). Other hand-picked coal particles from LSP sites 43 and 25R produced similar SEM images. EDS also detected Fe and S in molar abundances roughly the same as those of Si and Al.

Figure 6

Figure 7

Using organic petrography, Hagmann et al. (2019) demonstrated that the < 2 mm size fraction of the site 43 soil contained about 32 % detrital clay by volume. It is likely therefore that the aluminosilicate phases observed by SEM are clays. EDS spectra show approximately equal molar amounts of Si and Al, as well as an absence of K and Na. This suggests that the observed clays are most likely kaolinite (Welton, 1984). The iron and sulfur might be present as pyrite or a weathered derivative, however this was not confirmed petrographically.

The aluminosilicate clay encrustations present on the site 43 and 25R coal particles, such as those seen in Figures 6 and 7, have been interpreted as hallmarks of coal weathering in that oxidation allows clay minerals to better adhere to the coal surface (Xia et al., 2014, Xia & Yang, 2014). The LSP samples are from the top 10 cm of the soil profile. Thus, the coal particles were likely subjected to weathering over a half century or more, having been exposed to atmospheric O_2 in soil pore spaces, infiltrating meteoric water, seasonal temperature swings, and action by resident soil microbes. If the coal particles had been weathered chemically as well as physically,

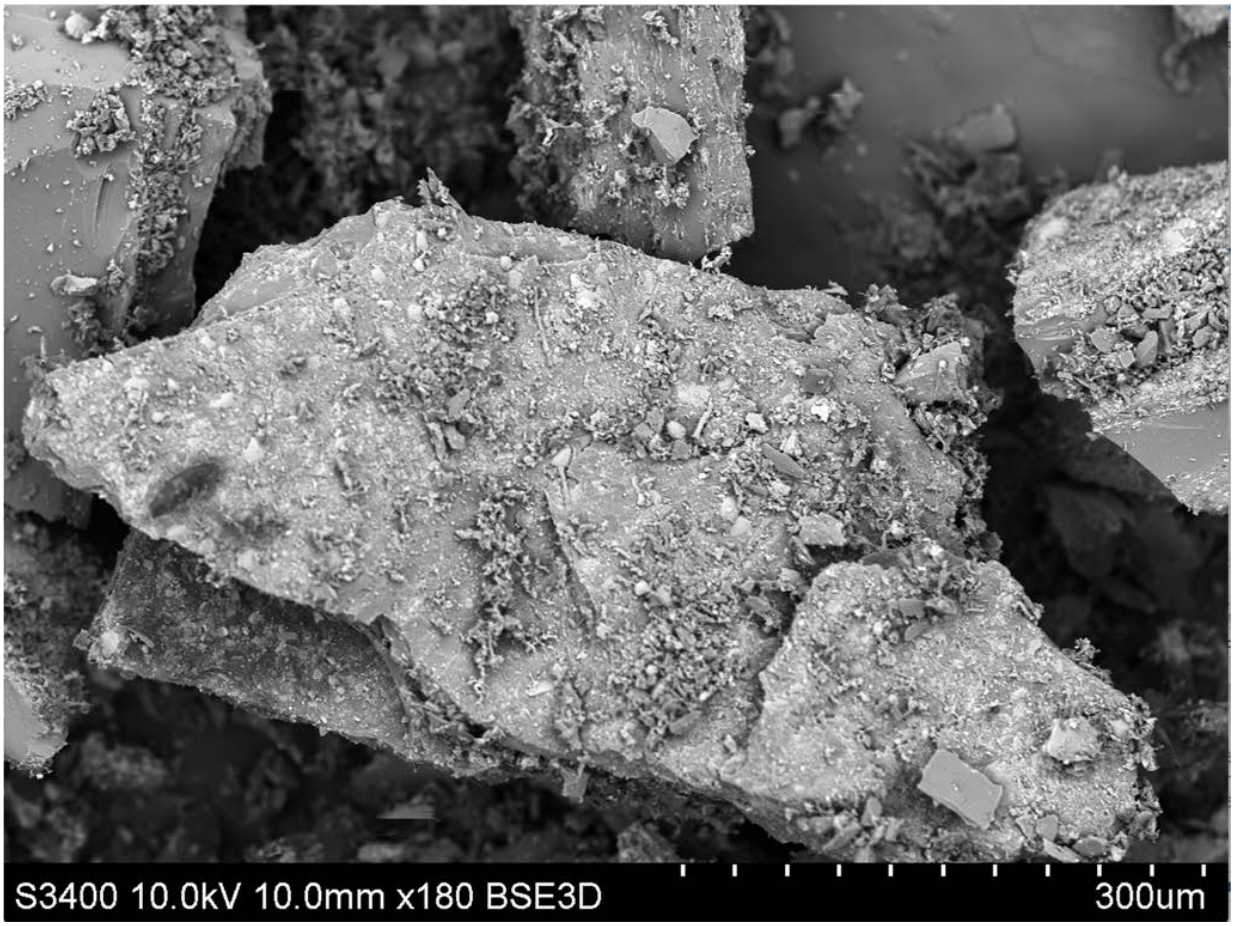

Figure 6. Scanning electron micrograph of fragments of a single wet-sieved (> 2 mm) and sonicated LSP 43 coal particle. Note surface encrustations. Scale bar is 300 μm.

(One column.)

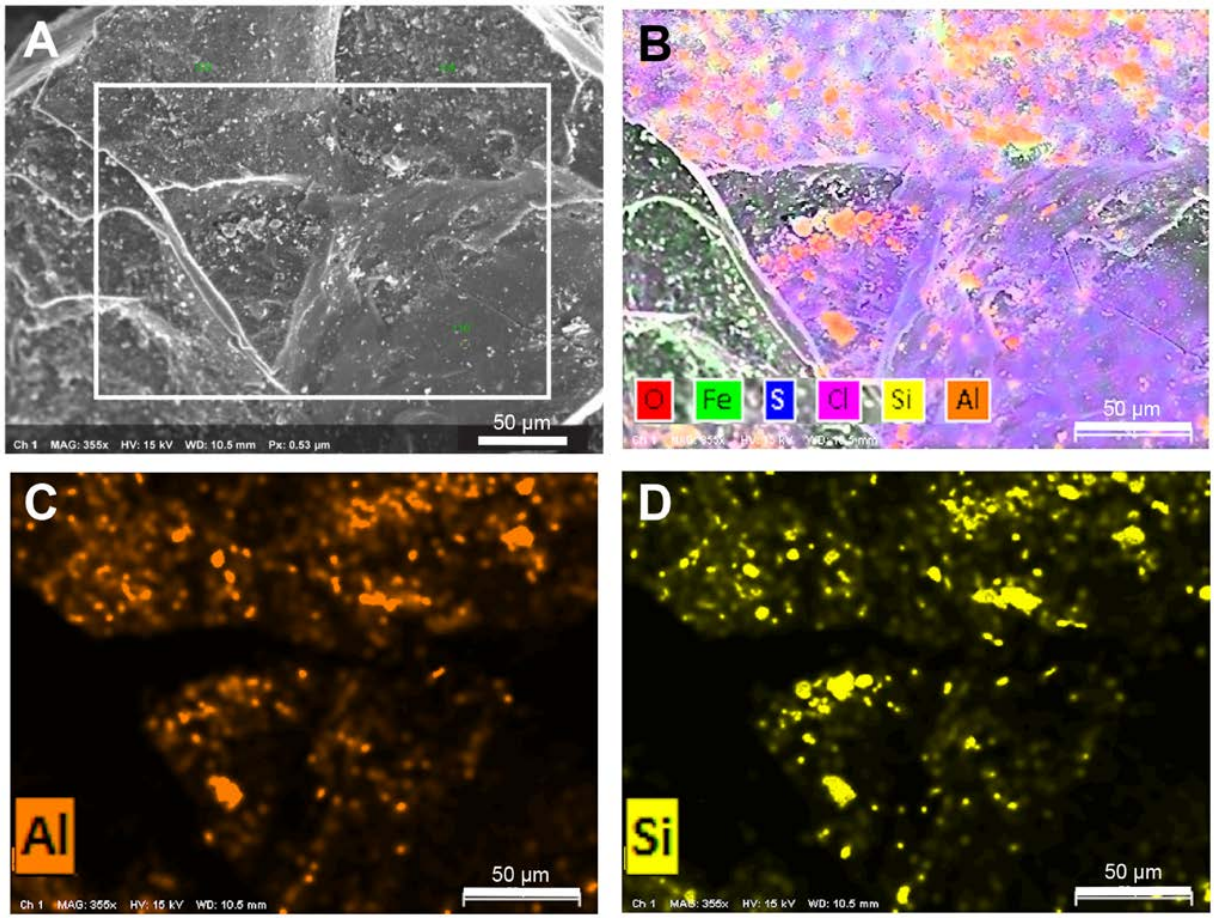

Figure 7. SEM EDS mapping images of a fragment of a single wet-sieved (>2 mm) and sonicated LSP 43 coal particle. Scale bars are 50 µm. (A) SEM image; box shows element mapping area for B-D. (B) Multi-element map (O, Fe, S, Cl, Si, Al) superimposed on SEM image. (C) Element map for aluminum. (D) Element map for silicon. Element mapping images indicate clay mineral platelets adhering to coal.

(Two column. Grayscale in print edition; color in online edition.)

their composition would obviously have been affected. The particles were therefore subjected to chemical analysis in part to determine if this indeed had been the case (Sec. 3.2).

3.2. Py-GC-MS of coal particles and plant material

The pyrolysis products of the vegetation detritus from site 43 included lignin marker compounds [methoxyphenols, labeled as chromatographic peaks L1-L15], polysaccharide derivatives [P1-P6], phenols [F1-F3], long-chain aliphatic hydrocarbons [^], steroids [S1, S2], and triterpenoids similar to β-amyrone [BAM] (Fig. 8A, Table 1). Ten coal particles were analyzed by Py-GC-MS. Nine of them had pyrograms resembling the one in Figure 8B, essentially showing only the simple monoaromatic hydrocarbons benzene [A1], toluene [A2], and alkylated benzenes [A3-A6]. Only one out of ten site 43 coal particles had a distinctly different pyrogram (Fig. 8C). This much more complex pyrolyzate, in addition to the monoaromatics [A1-A7], contained phenol and alkylated phenols [F1-F8], dibenzofuran [DBF], alkylated dibenzofurans [DBFx], parent and alkylated PAHs including naphthalenes [Nx], phenanthrenes [PHNx], fluorene [FLU], pyrenes [PYRx], and chrysenes [CHRx]. The alkylated PAHs were relatively more abundant than the parent compounds, and pristane predominated over phytane.

Figure 8

Table 1

The lignin and polysaccharide marker compounds present in the pyrolyzate of the plant material (Fig. 8A), which is comprised of roots and twigs, are those typical of vegetation and forest soil biomass (e.g., Saiz-Jiménez & de Leeuw, 1986; Hempfling & Schulten, 1990; Kuder & Kruge, 1998; Kuroda & Nakagawa-izumi, 2006). The steroids and triterpenoids likely derive

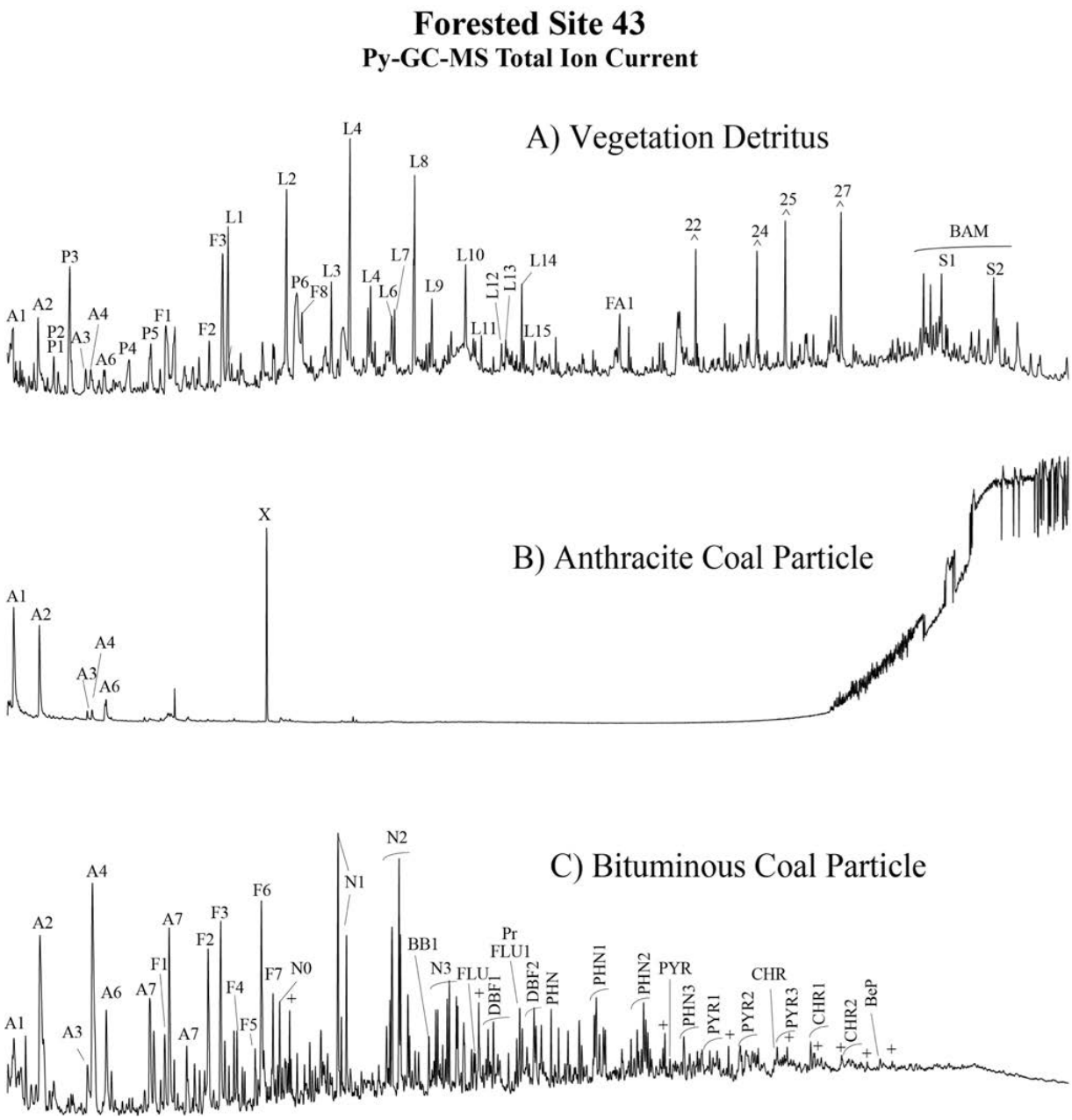

Figure 8. Py-GC-MS total ion current chromatograms of materials from the site 43 soil sample: (A) typical soil organic matter (roots & twigs) and (B, C) two coal particles hand-picked from the >2 mm size fraction after wet sieving and sonication. See Table 1 for peak identification.

(Two column.)

Table 1. Pyrolysis-GC-MS peak identification for Figures 8-10.

Aliphatic Hydrocarbons	
+	n-alkanes
^	n-alk-1-enes
pr	pristane
Monoaromatic Compounds	
A1	benzene
A2	toluene
A3	ethylbenzene
A4	meta- & para-xylene
A5	styrene
A6	ortho-xylene
A7	C3-alkylbenzene
A8	benzaldehyde
A9	benzonitrile
Polycyclic aromatic compounds	
Nx	naphthalenes
BBx	biphenyls
DBFx	dibenzofurans
PHNx	phenanthrenes
FLUx	fluorenes
FLA	fluoranthene
PYRx	pyrenes
BAN	benzo[a]anthracene
CHRx	chrysenes
BeP	benzo[e]pyrene
(x indicates extent of alkyl substitution)	
Phenols	
F1	phenol
F2	2-methylphenol
F3	3-methylphenol & 4-methylphenol
F4	2-ethylphenol
F5	2,4-dimethylphenol
F6	4-ethylphenol
F7	3-ethylphenol & 3,5-dimethylphenol
F8	vinylphenol
F9	trimethylphenol isomers
Polysaccharide markers	
P1	furan-3-one
P2	2-furancarboxaldehyde
P3	3-furancarboxaldehyde
P4	methylfuranone
P5	methylfurancarboxaldehyde
P6	benzenediol
Lignin markers	
L1	guaiacol
L2	methylguaiacol
L3	ethylguaiacol
L4	vinylguaiacol
L5	eugenol
L6	vanillin
L7	cis iso-eugenol
L8	trans iso-eugenol
L9	acetovanillone
L10	vinylsyringol
L11	prop-1-enyl syringol
L12	prop-2-enyl syringol (cis)
L13	syringaldehyde
L14	prop-2-enyl syringol (trans)
L15	acetosyringone
Fatty acids	
FA1	n-hexadecanoic acid
FA2	n-octadec-9-enoic acid
FA3	n-octadecanoic acid
Steroids	
S1	stigmastan-3,5-diene
S2	stigmasta-5-en-3-ol
S3	stigmasta-3,5-dien-7-one
S4	stigmasta-4-en-one
S5	stigmasta-4,22-dien-3one
Other	
BAM	terpenoids similar to β-amyrone ($C_{30}H_{48}O$) or derivative
DKDP	diketodipyrrole
X	contaminant introduced during processing

from the plant matter and/or soil microbes (Hagmann et al., 2019). Fresh and degraded plant materials obviously constitute important, non-contaminant soil components, which furthermore produce strong pyrolytic signatures. In their prior study, Hagmann et al. (2019) pyrolyzed whole LSP soils, yielding results in which the contaminant signals were mixed with those of the natural vegetation present. One objective of the present study is the isolation of the coal contaminant signatures from that of the plant material, for which the first step is the characterization of the individual components. The next step (Section 3.3) is the experimental attempt to isolate these soil constituents by density separation.

It was assumed that the coal particles hand-picked from the soil samples (Sec. 2.3) would include coals of different ranks since the historical record documents bulk transport of bituminous and anthracite by coal-fired locomotives (Anderson, 1984). One coal particle (Fig. 8B) produced simple alkylated benzenes nearly exclusively upon pyrolysis, consistent with previously documented anthracite coal pyrolyzates (Xu et al., 2017). Organic petrography indicated the presence of inertinite-dominant coal particles in soil samples from Site 43 (Hagmann et al., 2019) but inertinite pyrolysis products are considerably more complex (Stankiewicz et al., 1994a). Therefore, this coal particle and the other eight yielding similar pyrograms are all deemed to be anthracite by their distinctive pyrolytic fingerprint (although in the absence of confirmation by organic petrology or proximate and ultimate analysis). The sample shown in the SEM images (Figs. 6, 7) is one of these eight particles. About 70 % of the coal at this site was previously determined to be anthracite by petrographic examination (Hagmann et al., 2019), so it would not be surprising that most of the hand-picked coal particles in the present study would be anthracite.

Pyrolysis products from the remaining coal particle (Fig. 8C) closely resemble those of bituminous coal (Hatcher et al., 1992; Kruge & Bensley, 1994; Stankiewicz et al., 1994a; b; Laumann et al., 2011). These authors attest to the singular importance of oxygenated compounds in high-volatile bituminous coal pyrolyzates, in particular the phenols, as well as secondary amounts of dibenzofurans. These compounds are clearly evident in this particle's pyrolyzate [F1-F7, DBF1, DBF2]. Alkylnaphthalenes are also important components of bituminous coal pyrolyzates (Hatcher et al., 1992; Kruge & Bensley, 1994; Stankiewicz et al., 1994a) and are among the most abundant [N0-N3] in the present example (Fig. 8C). These same authors also demonstrated that pyrolytic phenols predominate when analyzing vitrinite of lower rank high volatile bituminous coals. However, in pyrolyzates of coals of increasing rank, the relative importance of the phenols is progressively reduced, while both parent and alkylated PAHs become more evident (Kruge & Bensley, 1994; Laumann et al., 2011). Although phenols [F1-F7] are very significant components in the present case (Fig. 8C), the prevalence of naphthalenes [N0-N3], and larger parent and alkyl-PAHs including the phenanthrenes [PAHx], pyrenes [PYRx], and chrysenes [CHRx] suggest that this is likely to be a higher rank bituminous coal. Previous petrographic examination (Hagmann et al., 2019) indicated that 17 % of the coal in the site 43 soil was medium volatile bituminous while only 8 % was high volatile. The particle in this case (Fig. 8C) is likely to be medium volatile based on its pyrolytic signature. Pyrolysis did not reveal marked evidence of chemical weathering, such as oxygenated PAHs.

3.3. Density separation of soil

Whole soils from vegetated site 43 and barren site 25R were separated into three fractions based on density (Fig. 5, Table 2). To achieve a clean signal for the coal Py-GC-MS

fingerprints, the plant material, predicted to be Fraction 1, needed to be separated from the coal particles, expected in Fraction 2, as explained in Section 3.2. The residue material anticipated in Fraction 3 was anticipated to confirm that the coal particles had been successfully isolated in Fraction 2. The site 25R soil yielded only 0.06 % by weight of light Fraction 1 while site 43 yielded 0.39 %. LSP site 43 had more of the intermediate Fraction 2 (3.10 %) compared to site 25R (0.89 %). For both sites, most of the material remained in the heavy third fraction (92.6 and 95.9 %, respectively, for 43 and 25R).

Table 2

Previous work (on the < 2 mm size fraction) indicated that the LSP soil samples were rich in organic matter (soil biomass plus coal, coke and char). Site 43 soil was found to consist of about 30 % by weight of organic matter, while 25R had about 11 % (Hagmann et al., 2019). Therefore, the low Fraction 1 and 2 yields (Table 2) appear incongruous at first glance. With bituminous coal and anthracite having specific densities of 1.32 and 1.47 g/mL, respectively (Flores, 2013; Wood et al., 1983), the KI solution with a density of 1.6 g/mL employed in the present experiment was expected to be adequate for the floatation of both types of coal. However, based on the SEM observations (Figs. 6, 7), stubbornly adhering mineral phases evidently precluded a complete isolation of coal fragments by density, relegating most of the material to the third (residual) fraction (Table 2). Adhering or embedded minerals increase the bulk density of the coal particles, perturbing the outcome of float-sink procedures (Garcia et al., 1991; Stankiewicz et al., 1994b; Suárez-Ruiz & Crelling, 2008). SEM examination of the residual fraction did indeed reveal abundant, widely-distributed mineral matter for both soil samples. A more rigorous attempt to isolate the organic materials from the minerals by a micronization pretreatment was beyond the scope of this project.

Table 2. Dry weight percentages of density fractions separated from whole soil of LSP Sites 43 and 25R. See text and Figure 5 for procedural details.

Soil	**Total soil dry weight**	**Fraction 1** (floated in DI water)	**Fraction 2** (floated in 1.6 g/mL KI_{aq})	**Fraction 3** (sank in 1.6 g/mL KI_{aq})
43	5.007 g	0.39 %	3.10 %	92.58 %
25R	5.046 g	0.06 %	0.89 %	95.94 %

3.4. Py-GC-MS of soil density fractions

To investigate their organic chemical composition in detail, whole soil and each density fraction were subjected to Py-GC-MS (Fig. 5). Results from the two field sites are presented separately.

3.4.1. Forested site 43 soil

Upon pyrolysis, forested site 43's whole soil revealed a predominance of simple alkylbenzenes and naphthalenes [A1-A7, N0-N3] (Fig. 9A). Notable minor components include polysaccharide and lignin marker compounds [P1-P3, L1], phenols [F1-F5], dibenzofurans [DBFx], PAHs [FLUx, PHNx, FLA, PYR, CHR], diketodipyrrole [DKDP] and long-chain *n*-alkanes [+]. Hagmann et al. (2019) noted a greater prevalence of polysaccharide and lignin markers, as well as phenols in site 43 soil pyrolyzates, but it must be kept in mind that they analyzed only the < 2 mm soil size fraction. The site 43 density Fraction 1 pyrolyzate is distinctly different from the whole soil, with lignin and polysaccharide markers dominant [L1-L15, P1-P6], along with phenols [F1-F8], diketodipyrrole [DKDP], fatty acids [FA1-FA3], long-chain *n*-alkenes [^], and sterols [S1, S2] (Fig. 9B).

Figure 9

The complex pyrolyzate of Site 43's Fraction 2 has an overwhelmingly aromatic signature (Fig. 9C). Significant compounds include monoaromatic hydrocarbons [A1-A7], phenols [F1-F8], naphthalenes [N0-N3], dibenzofurans [DBFx], and parent and alkylated PAHs [FLU1, PHNx, PYRx, CHRx, BeP]. *n*-Alkanes [+] and triterpenoids [BAM] are also noteworthy. In contradistinction, Fraction 3 produced mostly monoaromatic hydrocarbons [A1-

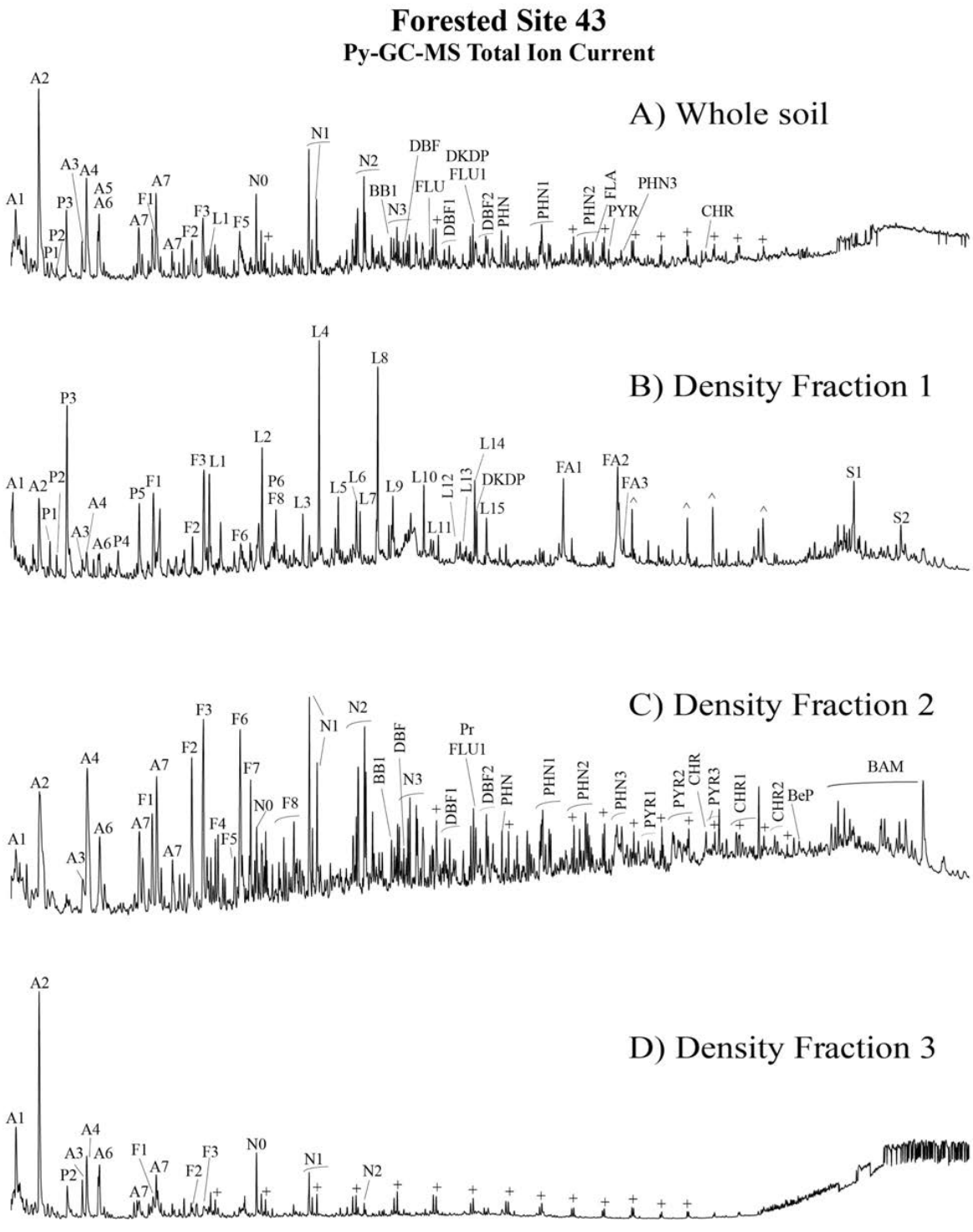

Figure 9. Py-GC-MS total ion current chromatograms. Forested LSP site 43: (A) whole soil, (B) Fraction 1 floated in DI water, (C) Fraction 2 floated in KIaq (1.6 g/mL), and (D) Fraction 3 sank in KIaq (1.6 g/mL). See Table 1 for peak identification.

(Two column)

A7] upon pyrolysis, accompanied by naphthalenes [N0-N2] with relatively minor phenols [F1-F3] and aliphatics [+] (Fig. 9D).

3.4.2. Barren site 25R soil

Site 25R is anomalously free of plant life (Fig. 4D), standing in stark contrast to its lushly vegetated surroundings (Fig. 4B, C). Hagmann et al. (2019) concluded that this is primarily due to the extraordinarily high heavy metal contamination of this narrow strip of land, formerly between train tracks (Fig. 2) which were removed when the railyard was closed in the 1960's (Gallagher et al., 2008a). The abundant coal particles in its soil are the subject of the present study.

Simple monoaromatic [A1-A9] and diaromatic [N0-N2, BB0] compounds with a trace of phenanthrene [PHN] comprise nearly all of site 25R's whole soil pyrolyzate (Fig. 10A). This site's < 2 mm soil size fraction previously pyrolyzed (Hagmann et al., 2019) yielded similar results but with a distinct shift towards the heavier aromatics. The first density fraction (Fig. 10B) produced a contrastingly complex distribution of pyrolysis products, in particular, monoaromatics [A1-A5], polysaccharide and lignin markers [P1-P6, L1-L15], phenols [F1-F8], diketodipyrrole [DKDP], fatty acids [FA1-FA3], and steroids [S1-S3].

Figure 10

The second density fraction's pyrogram is also complex, but it indicates a very different distribution of compounds (Fig. 10C). Monoaromatic [A1-A7] and diaromatic [N0-N3, BB1] hydrocarbons predominate, along with phenols [F1-F8]. Three to five-ring aromatic compounds are also in evidence, notably dibenzofurans [DBFx], phenanthrenes [PHNx], pyrenes [PYRx], chrysenes [CHRx], and benzo[*e*]pyrene [BeP]. Pristane [Pr] and *n*-alkanes [+] attest to a minor

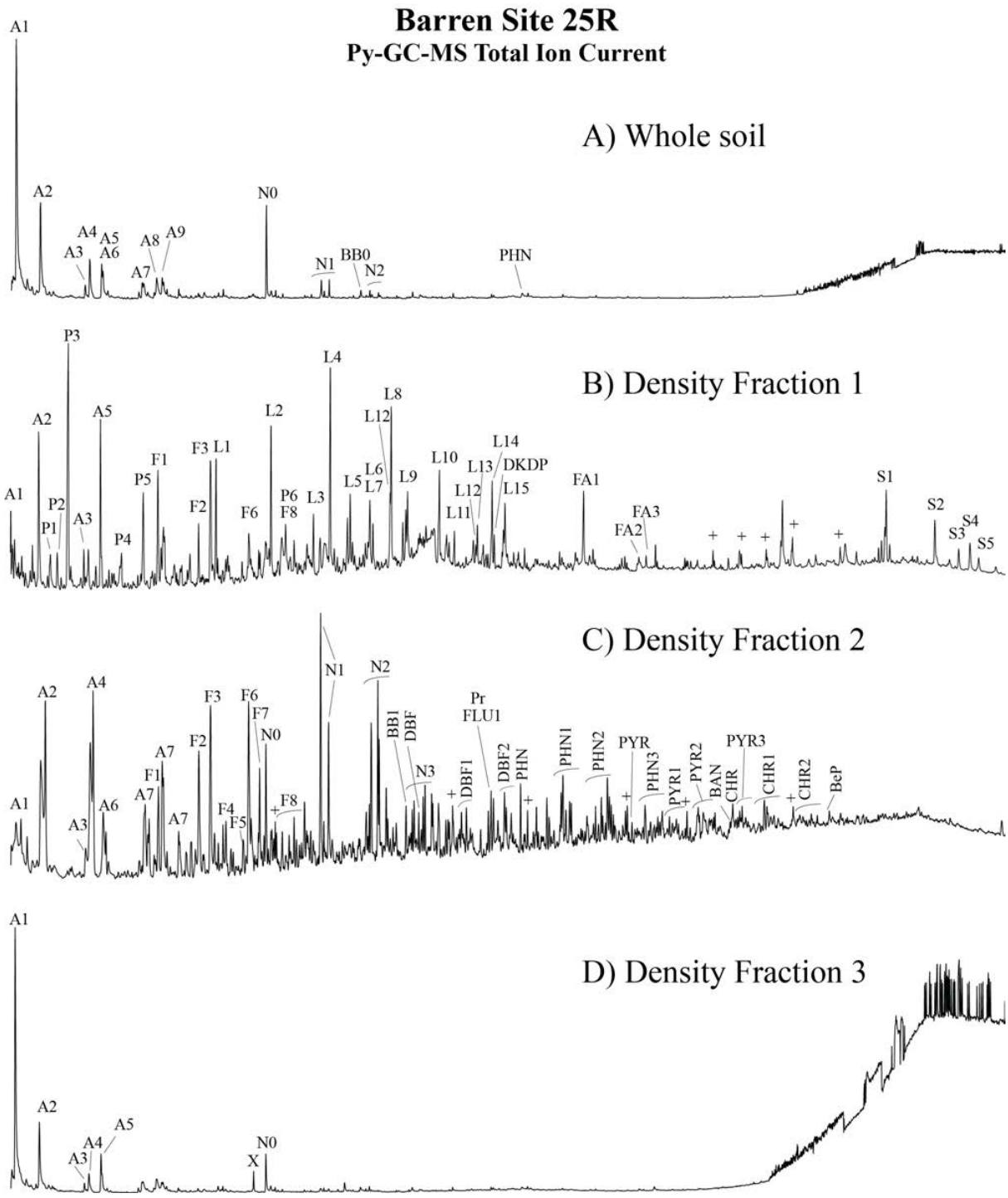

Figure 10. Py-GC-MS total ion current chromatograms. Barren LSP site 25R: (A) whole soil, (B) Fraction 1 floated in DI water, (C) Fraction 2 floated in KIaq (1.6 g/mL), and (D) Fraction 3 sank in KIaq (1.6 g/mL). See Table 1 for peak identification.

(Two column)

aliphatic component. The third, residual density fraction offered a very limited yield upon pyrolysis, mostly benzene [A1], a few other monoaromatics [A2-A5] and naphthalene [N0] (Fig. 10D).

3.4.3. Coal contamination in soil: Insights from Py-GC-MS of density fractions

A temperate forest soil is naturally rich in organic material, with roots, leaf litter, humus, fungi, and soil microbes. Forested soils in LSP have an anomalously high organic matter content: 30 % by weight in the case of site 43 compared to a natural background value of about 7.5 %, attributed to the additional burden of coal, coke and char contamination therein (Hagmann et al., 2019). Pyrolysis of the whole soil should therefore yield a complex mixture of products from all organic materials present, in proportion to the relative amounts of each type. Pyrolysis proneness should also be considered as wood and coal would yield abundant pyrolysis products, whereas coke and char would not. The combined effect can be seen in Figure 9A, showing aromatic hydrocarbons together with polysaccharide and lignin marker compounds in site 43's whole soil pyrolyzate.

The soil density fractionation experiment was undertaken in an attempt to separate the soil's organic components to improve the specificity of the subsequent chemical analyses. A critical factor was the isolation of the soil biomass from the fossil fuel contaminants present. The pyrolysis products of the first density fractions of both soils (Figs. 9B, 10B) closely resemble those of the soil vegetation detritus (Fig. 8A) in the predominance of lignin and polysaccharide markers and steroids. Therefore, plant matter is evidently the main component of the light fraction in both cases. The presence of diketodipyrrole [DKDP] – a known protein pyrolysis product (Orsini et al., 2017) – and relatively more fatty acids in the density fractions is

most likely due to soil microbial contributions. Although site 25R is barren of plant life, trace amounts of biomass were detected in its soil (Fig. 10B, Table 2), likely derived from the adjacent vegetated areas (Fig. 4D).

The second density fractions (Fraction 2) of both soils also produced very similar pyrolyzates (Figs. 9C, 10C). As described above, their pyrograms both show a predominance of mono- and diaromatic hydrocarbons, and phenols, along with parent and alkylated PAHs. The polysaccharide and lignin markers compounds characteristic of the vegetation debris are not detected. These distributions in turn closely resemble those derived from the medium volatile bituminous coal particle (Fig. 8C). It can be concluded that the second density fractions are predominantly bituminous coal. The triterpenoids [BAM] evident in soil 43's pyrogram likely indicate some, perhaps degraded, biomass contribution (Fig. 9C).

The third density fractions (Fraction 3) are alike in that their pyrolyzates contain predominantly simple monoaromatic hydrocarbons (Figs. 9D, 10D). They bear a strong resemblance to the anthracite pyrolysis products (Fig. 8B), indicating that anthracite is the primary pyrolyzable component therein. The presence of anthracite in this residual density fraction is likely due to the added mass of adhering mineral phases, as observed by SEM (Figs. 6, 7), precluding floatation in the 1.6 g/mL fluid employed. The site 43 pyrogram shows more of the alkylbenzenes and naphthalenes, along with trace amounts of phenols, suggesting that some bituminous coal is also present in this fraction, similarly burdened with mineral matter. The minor C_{11}-C_{26} *n*-alkanes detected (Fig. 9D) may arise from petroleum or coal tar-derived contamination in the soil adhering to mineral phases. Solvent extraction to test this supposition was beyond the scope of this project, but it is compatible with the conclusions of the prior study which did employ extraction and subsequent GC-MS (Hagmann et al., 2019). This prior work

also documented the presence of coke and char in these soils, confirmed during the hand-picking procedure of the present study (Sec. 2.3), but these materials yield little upon pyrolysis and thus escape detection by Py-GC-MS.

4. Conclusions

Analytical pyrolysis provided compelling evidence for the presence of biomass and bituminous and anthracite coal in the LSP soil density fractions. These insights should ideally be checked by organic petrography. The simple density separation experiment undertaken in this soil contamination study is shown to offer a helpful preparative technique, although not a rigorously quantitative one. The procedure could be improved by a micronization pretreatment step to more effectively permit separation of mineral components from the organic ones and by organic petrographic confirmation of the fraction compositions.

Of primary concern with the presence of coal at Liberty State Park is the potential environmental risk, principally due to coal's constituent PAHs. The abundant coal particles in LSP soils are the legacy of the park's past as major rail yard and port for the large-scale commercial transport and transfer of coal, powered by coal-fired steam locomotives, riding on rails supported by wooden crossties likely treated with coal tar-derived creosote. However, much of the LSP coal is anthracite and higher rank (medium volatile) bituminous. Extractable PAH content in coal decreases markedly with increasing coal rank (Stout and Emsbo-Mattingly, 2008; Laumann et al., 2011), therefore high rank coal particles in soil should pose less of an environmental concern on this basis. While the PAH-rich high volatile bituminous coal is proportionately less abundant at LSP, the extent to which it might be toxic or mutagenic to humans, plants, and animals is nonetheless linked to its degree of bioavailability. With the

evidently flourishing plant communities in great majority of the LSP brownfield zone, limited hot spots of acute contamination therein (Hagmann et al., 2019) likely demand the most intensive remediation efforts. Analysis of soil components by Py-GC-MS, particularly after a preparative density separation procedure, is shown to be effective in the environmental forensic and industrial archeological investigation of this urban brownfield. This detailed information about the nature of contaminants will help to inform future remediation efforts in the public interest.

Acknowledgements

We thank the National Science Foundation (NSF CBET 1603741) and the PSEG Institute for Sustainability Studies for the support for this study. We would also like to thank Laying Wu, Ph.D., for help using the scanning electron microscope, Matthew Cheung for assistance with historical research, and Mike Peters for field site photography. We sincerely thank Frank Gallagher, Ph.D. for facilitating access to Liberty State Park. One of us (MK) acknowledges the memory of his longtime friend and colleague, the late Professor Jack Crelling, coal petrographer and density separation pioneer.

References

Achten, C., Hofmann, T., 2009. Native polycyclic aromatic hydrocarbons (PAH) in coals – A hardly recognized source of environmental contamination. Sci. Total Environ. 407, 2461-2473.

Achten, C., Cheng, S., Straub, K.L., Hofmann T., 2011. The lack of microbial degradation of polycyclic aromatic hydrocarbons from coal-rich soils, Environ. Pollut. 159, 623-629.

Anderson, E., 1984. The Central Railroad of New Jersey's First 100 Years, 1849-1949. Center for Canal History and Technology, Canal Museum, Easton (PA).

Boggs, S., 2009. Petrology of Sedimentary Rocks, 2nd ed. Cambridge University Press, Cambridge.

Brooks, K.M., 2004. Polycyclic aromatic hydrocarbon migration from creosote-treated railway ties into ballast and adjacent wetlands. Madison, WI: U.S. Department of Agriculture, Forest Service, Forest Products Laboratory.

Crelling J.C., 1988. Separation and characterization of coal macerals including pseudovitrinite. 1988 lronmaking Conference Proceedings.

Crelling J. C., 1989. Separation and characterization of coal macerals: accomplishments and future possibilities. Am. Chem. Soc. Div. Fuel Chem. Prepr. 34, l, 249-255.

Dyrkacz G.R., Horwitz E.P., 1982. Separation of coal macerals. Fuel 61, 3-12.

Flores, R.M., 2014. Coal and coalbed gas: fueling the future. Elsevier, Waltham, MA.

Fabiańska M.J., Ciesielczuk, J., Misz-Kennan, M., Kruszewski, L., Kowalski, A., 2016. Preservation of coal-waste geochemical markers in vegetation and soil on self-heating coal-waste dumps in Silesia, Poland. Geochemistry 76, 211-226.

Gallagher, F.J., Pechmann, I., Bogden, J.D., Grabosky, J., Weis, P., 2008a. Soil metal concentrations and vegetative assemblage structure in an urban brownfield. Environ. Pollut., 153, 351-361.

Gallagher, F.J., Pechmann, I., Bogden, J.D., Grabosky, J., Weis, P., 2008b. Soil metal concentrations and productivity of *Betula populifolia* (gray birch) as measured by field spectrometry and incremental annual growth in an abandoned urban Brownfield in New Jersey. Environ. Pollut. 156, 699–706.

Gallagher, F.J., Goodey, N.M., Hagmann, D.F., Singh, J.P., Holzapfel, C., Litwhiler, M., Krumins, J.A., 2018. Urban re-greening: A case study in multi-trophic biodiversity and ecosystem functioning in a post-industrial landscape. Diversity 10, 119.

Garcia, A.B., Moinelo, S.R., Martinez-Tarazona, M.R., Tascón, J.M., 1991. Influence of weathering process on the flotation response of coal. Fuel 70, 1391-1397.

Hagmann, D.F., Goodey, N.M., Mathieu, C., Evans, J., Aronson, M.F.J., Gallagher, F.J., Krumins, J.A., 2015. Effect of metal contamination on microbial enzymatic activity in soil. Soil Biol. Biochem. 91, 291-297.

Hagmann, D.F., Kruge, M.A., Cheung, M., Mastalerz, M., Gallego, J.L.R., Singh, J.P., Krumins, J.A., Li, X., Goodey, N.M., 2019. Environmental forensic characterization of former rail yard soils located adjacent to the Statue of Liberty in the New York/New Jersey harbor. Sci. Total Environ. 690, 1019-1034. https://doi.org/10.1016/j.scitotenv.2019.06.495.

Hatcher, P.G., Faulon, J.L., Wenzel, K.A., Cody, G.D., 1992. A structural model for lignin-derived vitrinite from high-volatile bituminous coal (coalified wood). Energy Fuels 6, 813-820.

Hempfling R., Schulten H.R., 1990. Chemical characterization of the organic matter in forest soils by Curie point pyrolysis-GC/MS and pyrolysis-field ionization mass spectrometry. Org. Geochem. 15, 131-145.

Hindersmann, B., Achten, C., 2018. Urban soils impacted by tailings from coal mining: PAH source identification by 59 PAHs, BPCA and alkylated PAHs. Environ. Pollut. 242, 1217-1225.

Kruge M.A., 2015. Analytical pyrolysis principles and applications to environmental science, in: Barbooti, M. (Ed.), Environmental Applications of Instrumental Chemical Analysis. CRC Press, Boca Raton (FL), p. 533-569.

Kruge, M.A., Bensley, D.F., 1994. Flash pyrolysis-gas chromatography/mass spectrometry of Lower Kittanning vitrinites: Changes in the distributions of polyaromatic hydrocarbons as a function of coal rank, in: Mukhophadyay, P. K., Dow, W.G. (Eds.), Vitrinite Reflectance as a Maturity Parameter: Applications and Limitations. Amer. Chem. Soc. Symp. Series 570, p. 136-148.

Kruge M. A., Landais P., Bensley D. F., Stankiewicz B. A., Elie M., Ruau O., 1997. Separation and artificial maturation of macerals from Type II kerogen. Energy Fuels 11, 503-514.

Kruge M.A., Gallego J.L.R., Lara-Gonzalo A., Esquinas N., 2018. Environmental forensics study of crude oil and petroleum product spills in coastal and oilfield settings: Combined insights from conventional GC-MS, thermodesorption-GC-MS and pyrolysis-GC-MS, in: Stout S., Wang Z. (Eds.), Oil Spill Environmental Forensics Case Studies. Butterworth-Heinemann (Elsevier), Oxford (UK), pp. 131-156.

Krumins, J.A., Goodey, N.M., Gallagher, F.J., 2015. Plant–soil interactions in metal contaminated soils. Soil Biol. Biochem. 80, 224-231.

Kuder, T., Kruge, M.A., 1998. Preservation of biomolecules in sub-fossil plants from raised peat bogs - A potential paleoenvironmental proxy. Org. Geochem. 29, 1355-1368.

Kuroda, K., Nakagawa-izumi, A., 2006. Analytical pyrolysis of lignin: Products stemming from β-5 substructures. Org. Geochem. 37, 665-673.

Lara-Gonzalo A., Kruge M.A., Lores I., Gutiérrez B., Gallego J.L.R., 2015. Pyrolysis-GC-MS for the rapid environmental forensic screening of contaminated brownfield soil. Org. Geochem. 87, 9-20.

Laumann, S., Micić, V., Kruge, M.A., Achten, C., Sachsenhofer, R.F., Schwarzbauer, J., Hofmann, T., 2011. Variations in concentrations and compositions of polycyclic aromatic

hydrocarbons (PAHs) in coals related to the coal rank and origin. Environ. Pollut. 159, 2690-2697.

McDonald, T.T., 2018. N.J. to turn 240 acres of Liberty State Park into wildlife oasis. The Jersey Journal, January 11, 2018. https://www.nj.com/hudson/2018/01/nj_announces_massive_plan_to_restore_240_acres_of.html. Retrieved June 8, 2019.

Nádudvari Á., Fabiańska M.J., Marynowski L., Kozielska B., Konieczyński J., Smołka-Danielowska D., Ćmiel, S., 2018a. Distribution of coal and coal combustion related organic pollutants in the environment of the Upper Silesian Industrial Region. Sci. Total Environ. 628-629, 1462-1488.

Nádudvari, A., Marynowski, L., Fabiańska, M.J., 2018b. Application of organic environmental markers in the assessment of recent and fossil organic matter input in coal wastes and river sediments: A case study from the Upper Silesia Coal Basin (Poland). Int. J. Coal Geol. 196, 302-316.

Orsini, S., Parlanti, F, Bonaduce, I., 2017. Analytical pyrolysis of proteins in samples from artistic and archaeological objects. J. Anal. Appl. Pyrol. 124, 643-657.

Saiz-Jiménez, C., de Leeuw, J.W., 1986, Lignin pyrolysis productions: Their structures and their significance as biomarkers. Org. Geochem. 10, 869-876.

Singh, J.P., Ojinnaka, E.U., Krumins, J.A., Goodey, N.M., 2019a. Abiotic factors determine functional outcomes of microbial inoculation of soils from a metal contaminated brownfield. Ecotox. Environ. Safe. 168, 450-456.

Singh, J.P., Vaidya, B.P., Goodey, N.M., Krumins, J.A., 2019b. Soil microbial response to metal contamination in a vegetated and urban brownfield. J. Environ. Manage. 244, 313-319.

Smith, M.J., Flowers, T.H., Duncan, H.J., Alder, J., 2006. Effects of polycyclic aromatic hydrocarbons on germination and subsequent growth of grasses and legumes in freshly contaminated soil and soil with aged PAHs residues. Environ. Pollut. 141, 519-525.

Stankiewicz, B. A., Kruge M. A., Crelling, J. C., 1994a. Geochemical characterization of maceral concentrates from Herrin No. 6 coal (Illinois Basin) and Lower Toarcian shale kerogen (Paris Basin), in: Curnelle, R., Sévérac, J.-P. (Eds.), Pétrologie Organique, Recueil des Communications, Colloque International des Pétrographes Organiciens Francophones, Publ. Spéc., Bull. Centres Rech. Explor.-Prod. Elf Aquitaine, Vol. 18, p. 237-251.

Stankiewicz B.A., Kruge M.A., Crelling J.C., Salmon G.L., 1994b. Density gradient centrifugation: application to the separation of macerals of Type I, II and Ill sedimentary organic matter. Energy Fuels 8,1513-1521.

Stout, S.A., Emsbo-Mattingly, S.D., 2008. Concentration and character of PAHs and other hydrocarbons in coals of varying rank – Implications for environmental studies of soils and sediments containing particulate coal. Org. Geochem. 39, 801-819.

Suárez-Ruiz, I., & Crelling, J.C. (Eds.), 2008. Applied coal petrology: the role of petrology in coal utilization. Elsevier, Amsterdam. 398 p.

Wampler, T.P., 2007. Analytical pyrolysis: An overview, in: Wampler, T.P. (Ed.), Applied Pyrolysis Handbook, 2nd ed., CRC Press, Boca Raton (FL, USA), pp. 1–26.

Welton, J.E., 1984. SEM Petrology Atlas. Methods in Exploration Series No. 4, American Association of Petroleum Geologists, Tulsa (OK) USA. 240 p.

Wood, G.H., Kehn, T.M., Carter, M.D., Culbertson, W.C., 1983. Coal Resource Classification System of the US Geological Survey. Geological Survey Circular 891, U.S. Geological Survey, Denver (CO). 65 p.

Xia, W., Yang, J., & Liang, C., 2014. Investigation of changes in surface properties of bituminous coal during natural weathering processes by XPS and SEM. Appl. Surf. Sci. 293, 293-298.

Xia, W., Yang, J., 2014. Changes in surface properties of anthracite coal before and after inside/outside weathering processes. Appl. Surf. Sci. 313, 320-324.

Xu, J., Zhuo, J., Zhu, Y., Pan, Y., Yao, Q., 2017. Analysis of volatile organic pyrolysis products of bituminous and anthracite coals with single-photon ionization time-of-flight mass spectrometry and gas chromatography/mass spectrometry. Energy Fuels 31:730-737.

Yang, Y., Ligouis, B., Pies, C., Grathwohl, P., Hofmann, T., 2008a. Occurrence of coal and coal-derived particle-bound polycyclic aromatic hydrocarbons (PAHs) in a river floodplain soil. Environ. Pollut. 151, 121-129.

Yang, Y., Ligouis, B., Pies, C., Achten, C., Hofmann, T., 2008b. Identification of carbonaceous geosorbents for PAHs by organic petrography in river floodplain soils. Chemosphere 71, 2158-2167.

Figure and table captions

Figure 1. Index map showing location of Liberty State Park (LSP) in Jersey City (NJ), USA, the principal anthracite coal fields of Pennsylvania, and the former Central Railroad of New Jersey main line. Base map: Google Earth; coalfields: Pennsylvania Dept. of Environmental Protection; rail line: Anderson (1984).

Figure 2. The Central Railroad of New Jersey's rail yard and marine terminal in Jersey City as it appeared in a 1954 aerial image, overprinted with the location of the two soil samples (25R, 43)

presented in this study. At the time of the photograph, coal transport operations were largely confined to the zone seen in the lower part of the image, on the tracks leading to Pier 18. Note the locations of the passenger terminal and roundhouse. Base image: U.S. Geological Survey; identification of coal handling facilities: Anderson (1984); pier identification: Brooklyn Historical Society Archives.

Figure 3. Historical images of CRRNJ coal transport operations in the 1940's. (A) Loaded coal trains in Jim Thorpe, Pennsylvania (Fig. 1; town formerly known as Mauch Chunk). (B) Loaded coal cars approach Pier 18 in the Jersey City rail yard. View to the west showing the yard's track network (Fig. 2). (C) View of Pier 18's two coal dumping towers for transfer of coal from railcar to barge. View is to the west from the eastern end of the pier. (D) View to the northeast of Pier 18's coal dumpers. Note Ellis Island in the background. Photos: Anderson (1984); used with permission of the Delaware & Lehigh National Heritage Corridor, Inc., Easton (PA).

Figure 4. Appearance of Liberty State Park in 2017. (A) Aerial view towards the southwest showing the study area within the park. Note the former passenger rail and ferry terminal, partially restored but non-functioning, and the Liberty Science Center museum, built on the site of the former railroad roundhouse (Fig. 2). Photo: D. Hagmann. (B, C) Dense vegetation covers most of the study area. The top of the Liberty Science Center tower appears in C. (D) Soil sample 25R was collected from this anomalously barren strip within the study area. Photos B-D: M. Peters, Montclair State Univ.; used with permission.

Figure 5. Experimental flow chart. See section 2 for details. No vegetation detritus was picked from site 25R soil. * < 2 mm size fraction previously studied in detail (Hagmann et al., 2019).

Figure 6. Scanning electron micrograph of fragments of a single wet-sieved (> 2 mm) and sonicated LSP 43 coal particle. Note surface encrustations. Scale bar is 300 µm.

Figure 7. SEM EDS mapping images of a fragment of a single wet-sieved (>2 mm) and sonicated LSP 43 coal particle. Scale bars are 50 µm. (A) SEM image; box shows element mapping area for B-D. (B) Multi-element map (O, Fe, S, Cl, Si, Al) superimposed on SEM image. (C) Element map for aluminum. (D) Element map for silicon. Element mapping images indicate clay mineral platelets adhering to coal.

Figure 8. Py-GC-MS total ion current chromatograms of materials from the site 43 soil sample: (A) typical soil organic matter (roots & twigs) and (B, C) two coal particles hand-picked from the >2 mm size fraction after wet sieving and sonication. See Table 1 for peak identification.

Figure 9. Py-GC-MS total ion current chromatograms. Forested LSP site 43: (A) whole soil, (B) Fraction 1 floated in DI water, (C) Fraction 2 floated in KI_{aq} (1.6 g/mL), and (D) Fraction 3 sank in KI_{aq} (1.6 g/mL). See Table 1 for peak identification.

Figure 10. Py-GC-MS total ion current chromatograms. Barren LSP site 25R: (A) whole soil, (B) Fraction 1 floated in DI water, (C) Fraction 2 floated in KI_{aq} (1.6 g/mL), and (D) Fraction 3 sank in KI_{aq} (1.6 g/mL). See Table 1 for peak identification.

Table 1. Pyrolysis-GC-MS peak identification for Figures 8-10.

Table 2. Dry weight percentages of density fractions separated from whole soil of LSP Sites 43 and 25R. See text and Figure 5 for procedural details.